CMSC 754: Lecture 18
Introduction to Computational Topology

The introduction presented here is mainly based on Edelsbrunner and Harer's *Computational Topology*, while drawing doses of inspiration from Ghrist's *Elementary Applied Topology*; it is mostly self-contained, at the expense of brevity and less rigor here and there to fit the short span of one or two lectures. An excellent textbook to consult is Hatcher's *Algebraic Topology*, which is freely available online: `https://pi.math.cornell.edu/~hatcher/AT/AT.pdf`.

What is Topology? We are all familiar with Euclidean spaces, especially the plane $\mathbb{R}^2$ where we draw our figures and maps, and the physical space $\mathbb{R}^3$ where we actually live and move about. Our direct experiences with these spaces immediately suggest a natural *metric structure* which we can use to make useful measurements such as distances, areas, and volumes. Intuitively, a metric recognizes which pairs of locations are close or far. In more physical terms, a metric relates to the amount of energy it takes to move a particle of mass from one location to another. If we are able to move particles between a pair of locations, we say the locations are *connected*, and if the locations are close, we say they are *neighbors*. In every day life, we frequently rely more upon the abstract notions of *neighborhoods* and *connectedness* if we are not immediately concerned with exact measurements. For instance, it is usually not a big deal if we miss the elevator and opt to take the stairs, or miss an exit on the highway and take the next one; these pairs of paths are equivalent if we are not too worried about running late to an important appointment.

How do we develop our understanding of spaces without a metric structure? This brings to mind the more familiar setting of *graph theory*, which deals with abstract networks of nodes connected by edges. While we might picture a certain configuration of the nodes and their interconnections, we are not too fixated on the exact *positions* of the nodes nor their relative *distances*. Despite the underspecified *shape* or *realization* of the graph, we are still aware of other qualitative properties, such as the adjacency relation and the number of connected components, which are again easy to describe in terms of *neighborhoods* and *connectedness*. Specifically, those qualitative properties are *invariant* under arbitrary *deformations* as long as they preserve the *neighborhood structure*, i.e., the adjacency relation, of the graph.

Eulerian Paths. The foundations of graph theory are largely credited to Euler who established its first result by resolving the well-known *Eulerian path* problem in 1735. In its original form, the problem simply asked to find a path that crossed each of seven bridges exactly once; see Figure 1(left).

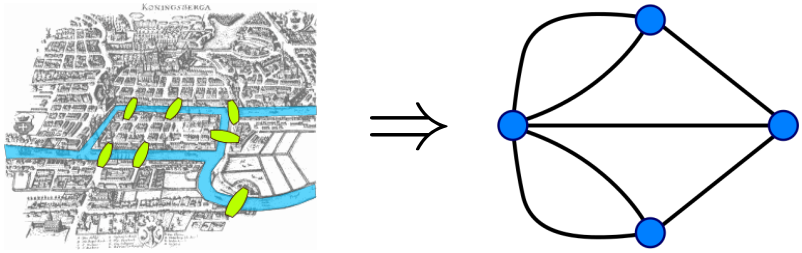

Fig. 1: Seven Bridges of Königsberg, and the origin of graph theory. (Figures from [1, 2])

Euler's *topological insight* was to recognize that the subpaths within each land mass are irrelevant to the solution. This allows one to consider the abstract setting provided by the usual graph model; see Figure 1(right). Next, observing how the path first enters into a node through an edge before leaving through a different edge, Euler correctly identified the issue with vertices of *odd degree*. In particular, an Eulerian path exists if and only if the graph has exactly zero or two nodes of odd degree. Euler later published the result under the title "The solution of a problem relating to the geometry of position," where the *geometry of position* indicates that it is about something more general than *measurements and calculations*.

As hinted in the previous example, one of the main uses of topological ideas is to identify an *obstruction* to the existence of an object.

Forbidden Graph Characterizations. If we cannot solve a problem on a given graph H, chances are we cannot solve it on any other graph G whenever G contains *something* that *looks like* H. To formalize this notion, define a *contraction* as the merging or *identification* of two adjacent vertices. We say that H is a *minor* of G if H can be obtained by a sequence of contractions, edge deletions, and deletion of isolated vertices. The equivalent theorems of Kuratowski (1930) and Wagner (1937) essentially state that a graph G is planar if and only if its minors include neither K_5 nor $K_{3,3}$, i.e., the complete graph on five nodes and the complete bipartite graph on six vertices; see Figure 2(a) and (b). Hence, the existence of a K_5 or $K_{3,3}$ minor is an *obstruction* to planarity. The Petersen graph shown in Figure 2(c), which serves as counterexample for many claims in graph theory, contains K_5 and $K_{3,3}$ as minors. Hence, the Petersen graph is not planar.

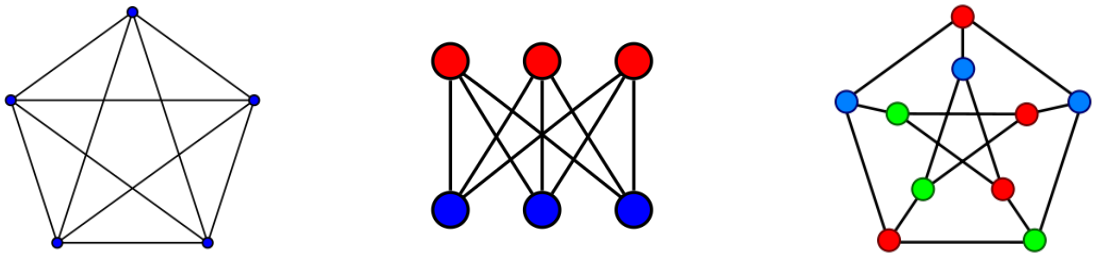

(a) K_5. (b) $K_{3,3}$. (c) 3-coloring of the Petersen graph.

Fig. 2: Graph minors and coloring. (Figures from [3, 4, 5])

Another example of obstruction is provided in the context of *graph coloring*, which has many applications in scheduling and distributed computing. Recall that a t-coloring of a graph is an assignment of one of t colors to each vertex such that no two adjacent vertices get the same color; see Figure 2(c). Clearly, a coloring of K_t requires at least t colors. One of the deepest unsolved problems in graph theory is the *Hadwiger conjecture* (1943) postulating that K_t minors are the only *obstruction* to the existence of colorings with fewer than t colors.

Beyond the discrete spaces commonly studied in graph theory, a *topological space* can be any set endowed with a *topology*, i.e., a *neighborhood structure*. The mathematical subject of *topology* is the formal study of properties of topological spaces which are *invariant* under *continuous functions*. Such properties are simply referred to as *topological invariants*.

Genus. Intuitively, the genus of a connected and orientable surface is the number of *holes* or *handles* on it; see Figure 3. It is a traditional joke that a topologist cannot distinguish his coffee mug from his doughnut; as both have genus one, they may be (continuously) deformed into one another and are in that sense *topologically equivalent*. In contrast, the mismatch in the genus is an *obstruction* to the existence of continuous mappings from spheres to tori.

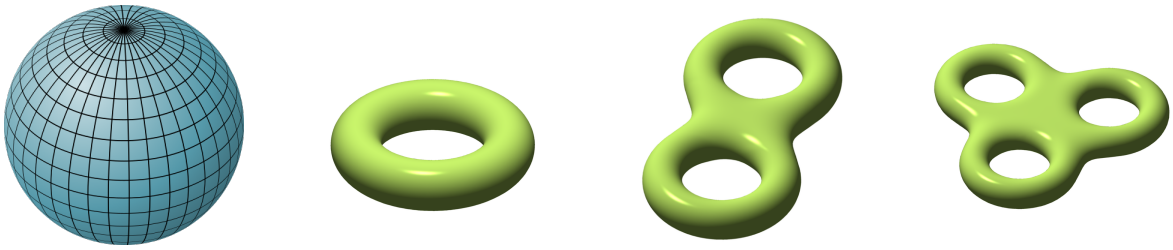

(a) $g = 0$. (b) $g = 1$. (c) $g = 2$. (d) $g = 3$.

Fig. 3: Genus of orientable surfaces. (Figures from [6, 7, 8, 9])

In relation to the previous examples, the *genus of a graph* is the smallest g such that the graph can be drawn without crossing on an orientable surface of genus g. Because the Earth is (locally) flat, *planar graphs* can be drawn on the sphere implying they have genus zero. More generally, the genus is one of the measures of complexity of the graph, and can be exploited to obtain faster algorithms for graphs with small genus. Alas, deciding whether a given graph has genus g is NP-complete.

While we may be interested in studying surfaces, or other topological spaces, we need simpler discrete structures to keep computations easy or at all feasible. This workaround does not allow us to compute everything we might have wanted, but it does provide very useful information. For example, the previous example showed how the genus can be used to classify surfaces. It turns out there is a closely related topological invariant which is more amenable to computation.

Euler's Polyhedron Formula. The following remarkable formula by Euler is considered, together with his resolution of the Seven Bridges of Königsberg problem, as the first two theorems in topology. Consider a *polyhedron* $P \subset \mathbb{R}^3$, and denote the number of vertices, edges, and faces of P by V, E, and F, respectively. The *Euler characteristic* χ is defined as:

$$\chi = V - F + E. \tag{1}$$

For any convex polyhedron P, we have that $\chi = 2$; see Figure 4. As the Euler characteristic is a topological invariant, one correctly anticipates that it also evaluates to 2 for the sphere.

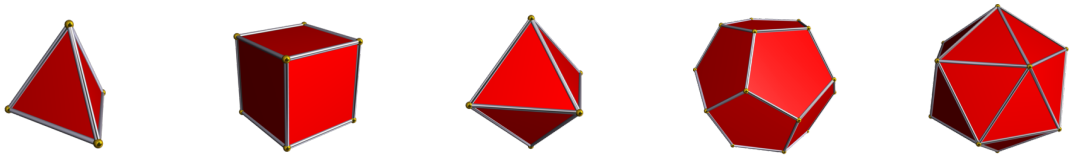

(a) $4 - 6 + 4$. (b) $8 - 12 + 6$. (c) $6 - 12 + 8$. (d) $20 - 30 + 12$. (e) $12 - 30 + 20$.

Fig. 4: Convex polyhedra with $\chi = 2$. (Figures from [10, 11, 12, 13, 14])

The previous example confirms the intuition that convex polytopes are suitable as *discrete approximations* to the sphere. In order to approximate arbitrary surfaces, which may not be convex, we are going to need more flexible structures.

Simplicial Complexes. You are probably familiar with triangular subdivisions of planar shapes, and the three-dimensional models suitable for rendering pipelines in computer games. Just a collection of vertices and connecting edges suffice to define a bare-bones *wireframe* that still captures the salient features of a shape; see Figure 5.

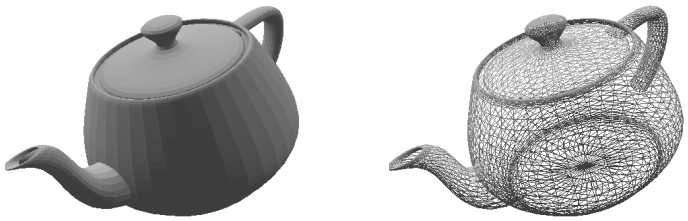

(a) Rendering all triangles. (b) Wireframe, edges only.

Fig. 5: The Utah teapot, arguably the *most important object in computer graphics history.*

It will prove useful to use a notation that easily generalizes to higher dimensions. We start with a set of points $S \subset \mathbb{R}^d$, for $d \geq 0$. We define a *p-simplex* σ as a subset of $p+1$ points in S, and we say that σ has *dimension* $\dim \sigma = p$. For a *geometric realization*, the simplex σ is the *convex hull* of $p+1$ affinely-independent points; see Figure 6. We write this as $\sigma = \text{conv}\{v_0, \ldots, v_p\}$. To capture the structure of the simplex, we define a *k-face* of σ is a simplex τ with (1) $\tau \subseteq \sigma$, and (2) $\dim \tau = k$ for $-1 \leq k \leq p$; we write this as $\tau \preceq \sigma$ and call σ a *coface* of τ. We say a (co)face of σ is proper if its dimension is different from $\dim \sigma$, and write $\partial\sigma$ for the proper faces of σ. Finally, the interior of σ is defined as $|\sigma| = \sigma - \partial\sigma$.

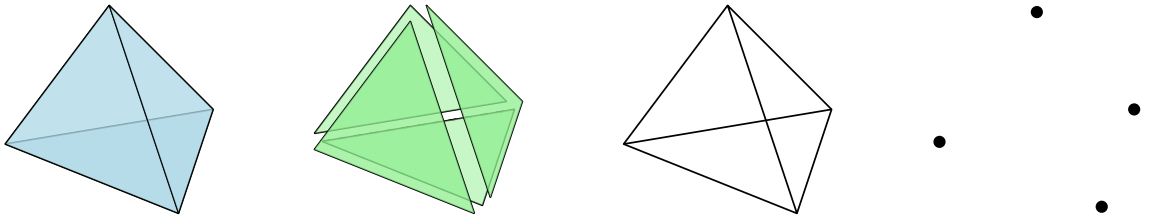

(a) A 3-simplex. (b) Four 2-simplices. (c) Six 1-simplices. (d) Four 0-simplices.

Fig. 6: The simplicial structure of a tetrahedron.

Suppressing realizations for a moment, we define an *abstract simplicial complex* K as a collection of simplices with the following *closure property.* Whenever a simplex σ appears in K, all faces of σ also appear in K. Similarly, we say that K is a *p-complex* with *dimension* $\dim K = \max_{\sigma \in K} \dim \sigma$ and *underlying space* $|K| = \cup_{\sigma \in K} |\sigma|$. For a geometric realization, we additionally require that for any two simplices $\sigma, \tau \in K$, we have that $\sigma \cap \tau \in K$. When this extra condition holds, we say that K is a *simplicial complex.* Every abstract simplicial complex of dimension p has a geometric realization, as a proper simplicial complex, in R^{2p+1}.

Before we can use simplicial complexes as proxies of topological spaces, we also need to approximate the continuous maps between such spaces through their simplicial proxies. We start by building some intuition as to how continuous maps act on spaces.

Continuous Maps. Imagine we have two surfaces X and Y, and a mapping $f : X \to Y$. In this case, f takes a point $x \in X$ to the corresponding point $y = f(x) \in Y$. Visually, y is where x ends up after going through some deformation that takes X to Y; see Figure 7. When do we consider such mappings to be continuous? Imagine you label two nearby points x_1 and x_2 on X and trace where they end up on Y. Once you identify the point $y_1 = f(x_1)$, where would you expect $y_2 = f(x_2)$ to be? For example, take x_1 and x_2 to be the the eyes of the cow.

Fig. 7: A continuous deformation of a cow model (X) into a ball (Y). (Figure from [15])

You are probably familiar with the notion of continuous functions from calculus which suggests we use an ε-neighborhood $V \subseteq Y$ around y and show that there is a corresponding $\delta = \delta(\varepsilon)$ such that all points in an δ-neighborhood $U \subseteq X$ around x are mapped by f into V, i.e., $f(U) \subseteq V$. In the particularly familiar context of a univariate function $g : \mathbb{R} \to \mathbb{R}$, the neighborhoods in question are immediately realized as *open intervals* of the form $(a, b) \subset \mathbb{R}$, where there is no shortage of intervals in the *continuum* which is $\mathbb{R}$ for us to choose from. Specifically, we require that $\lim_{\varepsilon \to 0} \delta(\varepsilon) = 0$; see Figure 8(a).

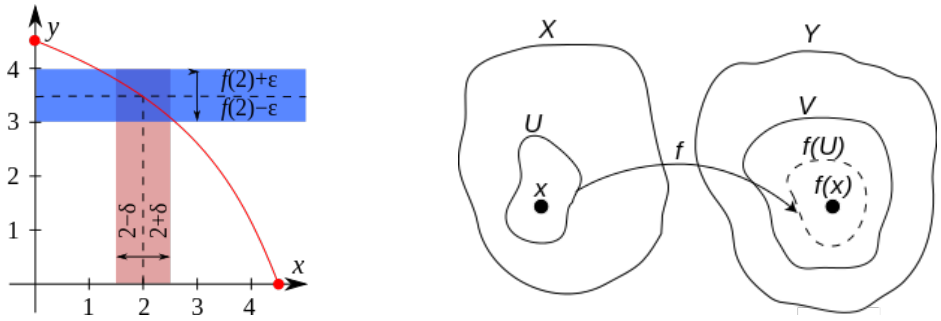

(a) Continuity at $x = 2$ by ε-δ. (b) Continuity at $x \in X$ using neighborhoods.

Fig. 8: Essentially equivalent definitions of continuous functions. (Figures from [16, 17])

It is plausible to conclude that neighborhoods, rather than the ε and δ, are all we need for continuity. Only that for general spaces, such as the surfaces X and Y, we have to work with their particular neighborhoods as specified by their respective topologies; see Figure 8(b). While not all topologies furnish neighborhoods as convenient as the intervals on the real line, a meaningful version of continuous maps can be defined for spaces with similar topologies.

Given our enhanced understanding of continuity, it is about time to formalize what we mean by *topologically equivalent* and *simplicial proxy*.

Homeomorphisms and Triangulations. A *homeomorphism* $f : X \to Y$ is a continuous function with a continuous inverse $f^{-1} : Y \to X$. Whenever such a homeomorphism f exists, we say that X and Y are *homeomorphic*, which literally translates to having the same shape. Applying this precise notion to our simplicial proxies, we say that a simplicial complex $\widehat{X}$ is a *triangulation* of X if its underlying space $|\widehat{X}|$ is homeomorphic to X.

We can now proceed to approximate a continuous mapping $f : X \to Y$ by a discrete mapping between triangulations $\widehat{f} : \widehat{X} \to \widehat{Y}$. But, what does it mean for such a mapping $\widehat{f}$ to be continuous?

Simplicial Neighborhoods. Take a point x in the underlying space $|\widehat{X}|$. To examine the continuity of $\widehat{f}$ at x, we need to consider the neighborhood of x on $|\widehat{X}|$. While x may belong to many simplices of $\widehat{X}$, there is a unique simplex that contains x in its *interior*; let us denote this simplex by $\sigma(x)$. If another point $x' \in \widehat{X}$ is a neighbor of x, it might be the case that $x' \in |\sigma(x)|$. However, we need to allow x' to go outside $|\sigma(x)|$ and reach farther parts of $\widehat{X}$.

Let us consider what lies beyond $|\sigma(x)|$. For example, if $\dim \widehat{X} = 3$ and $\sigma(x)$ is an edge with $\dim \sigma(x) = 1$, x' could start at x in $|\sigma(x)|$ and wander into a different simplex. Recalling the geometric realization, we consider an ε-neighborhood around x. We allow this neighborhood to expand over nearby *interior* points of adjacent simplices without crossing any boundaries, i.e., mimicking open intervals from calculus. For example, we do not connect x to the interior of an adjacent edge e unless there is a path through the interior of a common face or tetrahedron, i.e., a coface. As such, the neighborhood of x is contained in the cofaces of $\sigma(x)$.

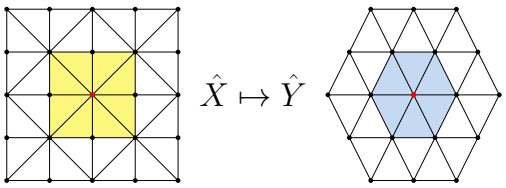

Fig. 9: One star in each of $\widehat{X}$ and $\widehat{Y}$. The star condition includes the image of one into the other.

The cofaces of a simplex $\sigma \in K$ constitute its *star*; we write this as $\mathrm{St}_K(\sigma) = \{\tau \in K \mid \sigma \preceq \tau\}$. Taking the union of all interior points, we define the *star neighborhood* as $N_K(\sigma) = \cup_{\tau \in \mathrm{St}_K(\sigma)} |\tau|$; see Figure 9. It will suffice for our purposes to consider the neighborhoods of vertices in $\widehat{X}$ and $\widehat{Y}$.

Star Condition. Recalling the definition of continuity, we require our maps $\widehat{f} : |\widehat{X}| \to |\widehat{Y}|$ to satisfy $\widehat{f}(N_{\widehat{X}}(v)) \subseteq N_{\widehat{Y}}(u)$ for all vertices $v \in \widehat{X}$ and some vertex $u = \phi(v) \in \widehat{Y}$; see Figure 9. This *star condition* has the following important consequence. Fix a point $x \in |\widehat{X}|$, and let $\sigma \in \widehat{X}$ and $\tau \in \widehat{Y}$ denote the unique simplices containing x and $\widehat{f}(x)$, respectively, in their interiors. Assuming σ is the p-simplex $[v_0, \ldots, v_p]$, we have by the definition of the star that $x \in N_{\widehat{X}}(\sigma) \subseteq N_{\widehat{X}}(v_i)$, for all $0 \leq i \leq p$; in fact $N_{\widehat{X}}(\sigma) = \cap_{i=0}^{p} N_{\widehat{X}}(v_i)$. Passing through $\widehat{f}$, the star condition implies that $\widehat{f}(x) \in \widehat{f}(N_{\widehat{X}}(\sigma)) \subseteq \cap_{i=0}^{p} N_{\widehat{Y}}(\phi(v_i)) \neq \emptyset$. By the same token, we get that $[\phi(v_0), \ldots, \phi(v_p)]$ is a simplex in $\widehat{Y}$ which must coincide with $\tau \ni \widehat{f}(x)$, i.e., $\widehat{f}(\sigma) = \tau$.

Instead of arbitrary continuous maps, there is great appeal to working with piecewise-linear maps on triangulations. In fact, the star condition was chosen to provide exactly that.

Simplicial Approximations. Assume that $\widehat{f} : |\widehat{X}| \to |\widehat{Y}|$ satisfies the star condition, and let $\phi_{\widehat{f}} : \text{Vert } \widehat{X} \to \text{Vert } \widehat{Y}$ be the associated *vertex map*. Fixing a p-simplex $\sigma = \text{conv}\{v_0, \ldots, v_p\}$, we may express any $x \in |\sigma|$ as a *linear combination* of the vertices. Using the so-called *barycentric coordinates*, we write $x = \sum_{i=0}^{p} \lambda_i v_i$, where $\lambda_i > 0 \; \forall i$. The expression can be extended to all vertices of K; letting $b_i(x) = \lambda_i$ for $0 \leq i \leq p$ and $b_i(x) = 0$ otherwise, we may write $x = \sum_i b_i(x) v_i$. Passing through $\phi_{\widehat{f}}$, we get that $\sum_i b_i(x) \phi_{\widehat{f}}(v_i) \in \phi_{\widehat{f}}(\sigma)$, where $\phi_{\widehat{f}}(\sigma)$ is a simplex in $\widehat{Y}$. As such, the vertex map $\phi_{\widehat{f}}$ induces a continuous, piecewise-linear *simplicial map* $x \mapsto \sum_i b_i(x) \phi_{\widehat{f}}(v_i)$. We will denote the induced simplicial map as $\widehat{f}_\Delta : \widehat{X} \to \widehat{Y}$. As both $\widehat{f}(x)$ and $\widehat{f}_\Delta(x)$ belong to the same simplex in $\widehat{Y}$, we call $\widehat{f}_\Delta$ a *simplicial approximation*, i.e., there is a smooth interpolation (or *homotopy*) to gradually change $\widehat{f}_\Delta$ into $\widehat{f}$.

While the star condition seems to provide all we need, it is only a convenient assumption we had to introduce. What about continuous maps from $|\widehat{X}|$ to $|\widehat{Y}|$ that the assumption fails to capture?

Subdivisions. Assume that a continuous map $\widehat{f} : |\widehat{X}| \to |\widehat{Y}|$ does not satisfy the star condition. Then, there must be a vertex $v \in \widehat{X}$ such that $\widehat{f}(N_{\widehat{X}}(v))$ is not contained in $N_{\widehat{Y}}(u)$ for *any* vertex $u \in \widehat{Y}$. Equivalently, $N_{\widehat{X}}(v)$ is not contained in any $\widehat{f}^{-1}(N_{\widehat{Y}}(u))$. In other words, $N_{\widehat{X}}(v)$ is relatively *too large*. Can we make the star of v *smaller* without changing $\widehat{f}$?

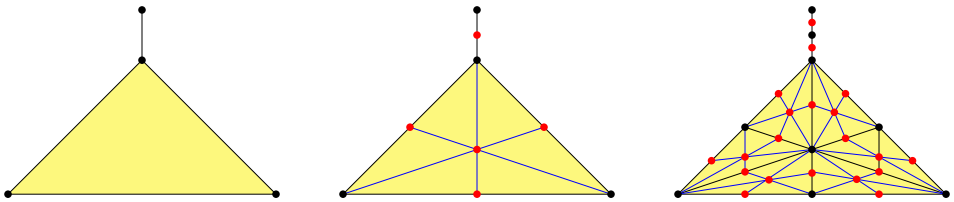

Fig. 10: Barycentric subdivisions of a triangle with an incident edge. New elements are highlighted.

It becomes clear that we need to keep $|\widehat{X}|$ intact, so that $\widehat{f}$ remains essentially the same, while making some stars smaller to satisfy the star condition. As the stars are defined by $\widehat{X}$, we seek a *finer* triangulation of $|\widehat{X}|$. One way to achieve that is to *subdivide* every simplex σ into smaller ones $\{\sigma'_i\}$ such that $|\sigma| = \cup \sigma'_i$. In particular, we make use of the *barycenter* of each simplex in $\widehat{X}$, which is defined as the average of its vertices. For $p = 1$ to $\dim \widehat{X}$, we insert the barycenter σ_c of each p-simplex σ as a new vertex, and form new p-simplices σ'_i by connecting σ_c to each $(p-1)$-simplex of the (subdivided) $(p-1)$-faces of $\partial\sigma$; denote this *barycentric subdivision* by Sd. A simple induction shows that every p-simplex is replaced by $(p+1)!$ new p-simplices; see Figure 10. More importantly, for any p-simplex σ, $\text{diam}(\sigma'_i) \leq \frac{p}{p+1} \text{diam}(\sigma)$. By repeating as needed, the diameters of all simplices are rapidly reduced such that the star neighborhoods of all vertices in $\text{Sd}^k \widehat{X}$ are covered by the pre-image of some vertex in $\widehat{Y}$. Specifically, $\text{Sd}^k \widehat{X}$ satisfies the star condition for a finite $k \geq 0$ and a simplicial approximation can then be defined on $\text{Sd}^k \widehat{X}$; this is known as the *simplicial approximation theorem*.

Having established triangulations as a viable discrete representation to approximate the topological spaces we will be studying, we now proceed to the computation of topological invariants. As in Euler's polyhedron formula, this computation boils down to a simple *counting*. However, as the structure of simplicial complexes is more complicated compared to polyhedra, we make use of a few tools from *algebra* to help keep track of our counts.

Simplicial Counting. Take a simplicial complex K, and let σ_1 and σ_2 be 2-simplices in K. In computing the Euler characteristic, we would need to count the triangles σ_1 and σ_2 before *subtracting* the number of edges. Now, it might be the case that σ_1 and σ_2 have an edge in common. An added difficulty is that a single triangle introduces *three* edges as its boundary.

To facilitate the counting and representation of boundaries, we will use special sets of simplices enhanced with two convenient operations.

Chains. We define the *p-chains* C_p as so-called *formal sums* of p-simplices: a p-chain c is written as $c = \sum_i a_i \sigma_i$, where σ_i ranges over all p-simplices in K and a_i simply indicates whether σ_i is included in c or not. To facilitate the counting of simplices, we define an *addition* operation. The *sum* of two chains $c_1 + c_2$ is the chain with all simplices in either c_1 or c_2, but not both, i.e., their symmetric difference. In other words, we choose a_i as *modulo 2 coefficients*.

The algebraic framework we are about to develop will compensate for the lack of geometric visuals with greater expressive power, as will prove essential to our computations.

Algebra I. A *group* $(A, \bullet)$ is a set A together with a *binary operation* $\bullet : A \times A \to A$, meaning that A is *closed* under the action of $\bullet$. We further require that $\bullet$ is *associative* so that for all $\alpha, \beta, \gamma \in A$ we have that $\alpha \bullet (\beta \bullet \gamma) = (\alpha \bullet \beta) \bullet \gamma$. Finally, we require an *identity element* $\omega \in A$ such that $\alpha + \omega = \alpha$ for all $\alpha \in A$. If, in addition, $\bullet$ is *commutative*, we have that $\alpha \bullet \beta = \beta \bullet \alpha$ for all $\alpha, \beta \in A$, and we say the group $(A, \bullet)$ is *abelian*.

Using this new language, we say that $(C_p, +)$ is an abelian group. In particular, if K has n_p p-simplices, then $(C_p, +)$ is (*isomorphic* to) the set of binary vectors of length n_p with the usual exclusive-or operation $\oplus$. Hence, $(C_p, +)$ is not just any group; *it is a vector space!*

Boundary Maps. By our definition of chains, any p-simplex $\sigma \in K$ also belongs to the chain group C_p. As the boundary of σ is a collection of $(p-1)$-simplices, it will be convenient to express the boundary *in one shot* as an element in C_{p-1}. Letting $\sigma = [v_0, \ldots, v_p]$ we write:

$$\partial_p \sigma = \sum_{i=0}^{p} [v_0, \ldots, \widehat{v_i}, \ldots, v_p], \tag{2}$$

where $\widehat{v_i}$ indicates that v_i is excluded in the corresponding $(p-1)$ face. We can also take the boundary of a collection of p-simplices, i.e., a p-chain, to obtain the sum of their boundaries as a single $(p-1)$-chain. We denote this mapping by $\partial_p : C_p \to C_{p-1}$, and write $\partial_p c = \sum_i a_i \partial_p \sigma_i$.

Naturally, every chain group C_p gets its own boundary map ∂_p, though we often drop the subscript of ∂_p as we have been doing already with addition and summation. The combined action of those two operators gives rise to a rich algebraic structure essential to our computations.

Algebra II. A mapping $\delta : (A, \bullet) \to (B, \odot)$ is called a *homomorphism* if it commutes with the group operation, i.e., $\delta(\alpha \bullet \alpha') = \delta\alpha \odot \delta\alpha'$ for all $\alpha, \alpha' \in A$. (Note the switch from $\bullet$ to $\odot$.)

It is easy to verify that $\partial_p(c + c') = \partial_p c + \partial_p c'$ for all $c, c' \in C_p$, i.e., ∂_p is a homomorphism. Recalling the simplicial structure depicted in Figure 6, we use the boundary homomorphisms to arrange our p-chain groups into a *chain complex* that we write as

$$\dots \xrightarrow{\partial_{p+2}} C_{p+1} \xrightarrow{\partial_{p+1}} C_p \xrightarrow{\partial_p} C_{p-1} \xrightarrow{\partial_{p-1}} \dots \xrightarrow{\partial_0} 0. \tag{3}$$

Effectively, we have replaced the simplicial complex with a sequence of algebraic modules, i.e., the chain complex. The added algebraic structuring of our chains quickly becomes useful for computation. Building upon the familiar language of vector algebra, we obtain a particularly convenient expression.

Boundary Matrices. Letting n_p denote the number of p-simplices, we saw how we can think of the chain group $(C_p, +)$ as the vector space $(\{0,1\}^{n_p}, \oplus)$. As the mapping $\partial_p : C_p \to C_{p-1}$ is well-defined, we can think of it in turn as a mapping $\partial_p : \{0,1\}^{n_p} \to \{0,1\}^{n_{p-1}}$ between vectors. Whenever a p-simplex is included in a p-chain c, we know that all $(p-1)$-simplices on its boundary contribute to the $(p-1)$-chain $\partial_p c$. Letting $\{\sigma_i\}_i$ and $\{\tau_j\}_j$ denote the sets of p-simplices and $(p-1)$-simplices, respectively, we write $c = \sum_i a_i \sigma_i$ and $\partial_p c = \sum_i a_i \partial_p \sigma_i = \sum_j b_j \tau_j$. Rearranging, we get that $b_j = \sum_i \partial_p^{j,i} a_i$, where $\partial_p^{j,i}$ is 1 if $\tau_j \prec \sigma_i$ and 0 otherwise. If we think of $[\partial_p^{j,i}]_i$ as a *column vector* for each j and the p-chain c as another column vector $[a_i]_i$, we recognize b_j as an *inner product*. Collecting all the vectors $[\partial_p^{j,i}]_{i,j}$ into a *boundary matrix*, we realize the boundary mapping as a *linear transformation* between vector spaces.

$$\partial_p c = \begin{bmatrix} b_1 \\ b_2 \\ \vdots \\ b_{n_{p-1}} \end{bmatrix}, \qquad \partial_p = \begin{bmatrix} \partial_p^{1,1} & \partial_p^{1,2} & \cdots & \partial_p^{1,n_p} \\ \partial_p^{2,1} & \partial_p^{2,2} & \cdots & \partial_p^{2,n_p} \\ \vdots & \vdots & \ddots & \vdots \\ \partial_p^{n_{p-1},0} & \partial_p^{n_{p-1},2} & \cdots & \partial_p^{n_{p-1},n_p} \end{bmatrix}, \qquad c = \begin{bmatrix} a_1 \\ a_2 \\ \vdots \\ a_{n_p} \end{bmatrix} \tag{4}$$

With the aid of these algebraic tools, we can now start using chains and see what comes out.

Boundaries and Cycles. Unlike the whole convex polytopes considered in Euler's equation, the chains we defined may correspond to an entire simplicial complex or just a subset of its simplices. While some of the chains carry useful information about the complex, many do not. Let us examine the 1-chains on triangulations of surfaces like the ones shown in Figure 3. There are many chains that cannot help us distinguish the sphere from any of the tori, e.g., the boundary of a single triangle. In contrast, other types of chains only arise if there is a handle; they include edges that *wrap around* one or more handles. We call that latter type *cycles*. How do we extract the number of handles from these cycles?

It is easy to see a cycle, but our computations will benefit from an algebraic characterization. If α is a 1-cycle, it consists of a set of vertices each shared by two edges. It follows that $\partial_1 \alpha$ counts each vertex twice *modulo 2* yielding 0. But, the same could be said about the boundary of any set of triangles whether it wraps around a handle or not. Hence, we distinguish two subsets of p-chains that have *no boundary*: those that arise as the boundary of some $(p+1)$-chain under the action of ∂_{p+1} are the *p-boundaries* B_p, and the rest are the *p-cycles* Z_p.

As outlined above, the *fundamental lemma of homology* asserts that $\partial_p \partial_{p+1} c = 0$ for every integer p and all chains $c \in C_{p+1}$. Furthermore, as ∂_p commutes with addition, both B_p and Z_p are *subgroups* of C_p, where B_p is in turn a subgroup of Z_p.

Multiplicity of Representation. There would typically be multiple 1-cycles that wrap around a single handle. Some of those cycles are *minimal*, containing only the edges that wrap around the handle, while others contain extra 1-boundaries that carry no additional information. Namely, for any $\alpha \in Z_p$ and $\beta \in B_p$, we have that $\alpha' = \alpha + \beta \in Z_p$.

The above discussion suggests that we need to recognize *equivalent* cycles while ignoring the contribution of any boundaries. To formalize this notion, we need a few more tools from algebra.

Algebra III. Given a group $(A, \bullet)$ and a subgroup B, we define an *equivalence relation* that identifies a pair of elements $\alpha, \alpha' \in A$ whenever $\alpha' = \alpha \bullet \beta$ for some β in B. The equivalence relation partitions A into *equivalence classes* or *cosets*; the coset $[\alpha]$ consists of all the elements of A identified with α. Then, the collection of cosets, together with the operator $\bullet$, give rise to the *quotient group* A/B of the elements in A *modulo* the elements in B.

Before we apply quotients, we recall that the *order* of a group is the total number of elements, and for abelian groups, like p-chains, the *rank* is the cardinality of a maximal linearly independent subset, i.e., the number of p-simplices.

Homology Groups. We define the p-th *homology group* H_p as Z_p/B_p. Now, to count the number of p-holes, we seek to compute the rank of H_p; this rank is known as the p-th *Betti number*

$$\beta_p = \text{rank } H_p = \text{rank } Z_p - \text{rank } B_p. \tag{5}$$

The computation of the Betti numbers relies on the following fundamental theorem in algebra.

Algebra IV. Let V and W be vector spaces and $T : V \to W$ be a *linear transformation*. We define the *kernel* of T as the subspace of V, denoted $\text{Ker}(T)$ of all vectors v such that $T(v) = 0$. The remaining elements $v \in V$ for which $T(v) \neq 0$ are mapped to a subspace of W; the *image* of T. The *rank-nullity theorem* states that $\dim V = \dim \text{Image}(T) + \dim \text{Ker}(T)$.

In the context of p-chains, we get that Z_p is the kernel of ∂_p, while B_{p-1} is its image. Hence, $\text{rank } C_p = \text{rank } Z_p + \text{rank } B_{p-1}$. Note that $B_{-1} = 0$, and for a d-dimensional complex $Z_{d+1} = 0$.

The Euler Characteristic (Redux). Recalling the alternating sum in Euler's polyhedron formula, we can now use the Betti numbers to derive the generalized *Euler-Poincaré formula*.

$$\begin{aligned}
\chi &= \sum_{p \geq 0} (-1)^p \text{ rank } C_p = \sum_{p \geq 0} (-1)^p (\text{rank } Z_p + \text{rank } B_{p-1}) \\
&= (\text{rank } Z_0 + \cancel{\text{rank } B_{-1}}) - (\text{rank } Z_1 + \text{rank } B_0) + (\text{rank } Z_2 + \text{rank } B_1) - \dots \\
&= (\text{rank } Z_0 - \text{rank } B_0) - (\text{rank } Z_1 - \text{rank } B_1) + (\text{rank } Z_2 - \text{rank } B_2) - \dots \\
&= \sum_{p \geq 0} (-1)^p (\text{rank } Z_p - \text{rank } B_p) \\
&= \sum_{p \geq 0} (-1)^p \beta_p.
\end{aligned} \tag{6}$$

A remarkable fact is that homology groups do not depend on the triangulation used, i.e., they are indeed *topological invariants*. Hence, the sequence of Betti numbers reveals important qualitative features of the underlying space. Now, all that remains is to compute the ranks as in Equation 5.

Matrix Reduction. As discussed above, recognizing Z_p as $\text{Ker}(\partial_p)$ we seek to compute the rank of the matrix ∂_p of dimensions rank $C_{p-1} \times$ rank C_p; see Equation 4. Using essentially the *Gaussian elimination* algorithm, we can *reduce* the matrix ∂_p *without changing its rank* by a series of transformations, i.e., *row and column operations*, into the *Smith normal form*; see Figure 11. As we work with modulo 2 coefficients, we obtain an initial segment of the diagonal being 1 and everything else being 0. Namely, the leftmost rank B_{p-1} columns have 1 in the diagonal, and the rightmost rank Z_p columns are zero. By processing all boundary matrices, we can extract the Betti numbers as the differences between the ranks $\beta_p =$ rank $Z_p -$ rank B_p. By keeping track of the reducing transformations, we can also obtain the bases of the boundary and cycle groups as subspaces of their respective chain groups.

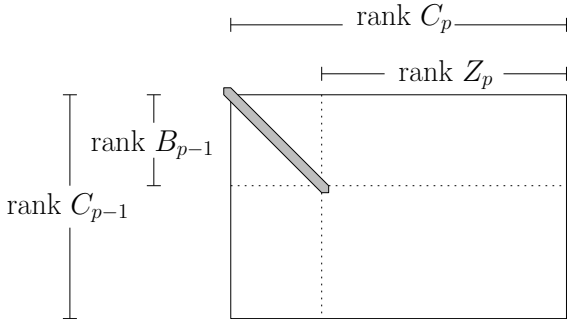

Fig. 11: Reducing the boundary matrix ∂_p to the Smith normal form.

Beyond the topological invariants of the spaces themselves, topology is also concerned with the invariants of maps between spaces.

Functoriality. Given two simplicial complexes $\widehat{X}$ and $\widehat{Y}$, a simplicial map $\widehat{f}_\Delta : \widehat{X} \to \widehat{Y}$ induces a map from the p-chains of $\widehat{X}$ to the p-chains of $\widehat{Y}$, which we denote by $\widehat{f}_\# : C_p(\widehat{X}) \to C_p(\widehat{Y})$. Letting $\partial_{\widehat{X}}$ and $\partial_{\widehat{Y}}$ denote the boundary maps for $\widehat{X}$ and $\widehat{Y}$, respectively, we get that the induced map commutes with the boundary maps, i.e., $\widehat{f}_\# \circ \partial_{\widehat{X}} = \partial_{\widehat{y}} \circ \widehat{f}_\#$. This can be expressed as a *commutative diagram* where all directed paths from one node to another are equivalent.

$$\begin{array}{ccccccccc} \dots & \xrightarrow{\partial_{\widehat{X}}} & C_{p+1}(\widehat{X}) & \xrightarrow{\partial_{\widehat{X}}} & C_p(\widehat{X}) & \xrightarrow{\partial_{\widehat{X}}} & C_{p-1}(\widehat{X}) & \xrightarrow{\partial_{\widehat{X}}} & \dots \\ & & \downarrow \widehat{f}_\# & & \downarrow \widehat{f}_\# & & \downarrow \widehat{f}_\# & & \\ \dots & \xrightarrow{\partial_{\widehat{Y}}} & C_{p+1}(\widehat{Y}) & \xrightarrow{\partial_{\widehat{Y}}} & C_p(\widehat{Y}) & \xrightarrow{\partial_{\widehat{Y}}} & C_{p-1}(\widehat{Y}) & \xrightarrow{\partial_{\widehat{Y}}} & \dots \end{array} \tag{7}$$

As the induced map $\widehat{f}_\#$ commutes with the boundary maps, it maps boundaries to boundaries and cycles to cycles. Consequently, $\widehat{f}_\#$ induces a map between homology groups, which we denote by $H(\widehat{f}) : H_p(\widehat{X}) \to H_p(\widehat{Y})$. This map $H(\widehat{f})$ on homology is an *algebraic reflection* of the continuous map $\widehat{f} : |\widehat{X}| \to |\widehat{Y}|$; it is a form of *functoriality* as studied in category theory.

Important applications of functoriality involve a map $f : Y_1 \to Y_2$ that *factors through a map* to X as shown in Figure 12. If the homologies of Y_1 and Y_2 are known, then we can use the induced homomorphisms to make inferences about the homology of X.

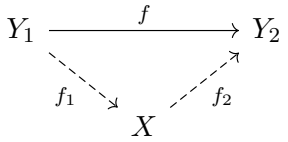

Fig. 12: $f : Y_1 \to Y_2$ with $f = f_2 \circ f_1$ where $f_1 : Y_1 \to X$ and $f_2 : X \to Y_2$.

To demonstrate this powerful proof technique, we present a remarkable and far-reaching result.

Brouwer Fixed-Point Theorem. Consider a self-map of the closed unit disc $f : \mathbb{D} \to \mathbb{D}$. A *fixed point* of f is any point $x \in \mathbb{D}$ such that $f(x) = x$. We will show that every *continuous* self-map of $\mathbb{D}$ must have a fixed point!

Assume for contradiction that $f : \mathbb{D} \to \mathbb{D}$ is continuous and has no fixed points. It would follow that for any $x \in \mathbb{D}$ there is a well-defined line passing through x and $f(x) \neq x$. Define $r(x)$ as the intersection of the ray from x towards $f(x)$ and $\partial\mathbb{D}$, i.e., the unit circle bounding the disk $\mathbb{D}$; see Figure 13. Hence, we implicitly defined $r : \mathbb{D} \to \partial\mathbb{D}$ using the self-map f. As f is continuous, so is r. In addition, $r(x) = x$ for all $x \in \partial\mathbb{D}$, i.e., r is a *retraction*. Denoting the inclusion of $\partial\mathbb{D}$ into $\mathbb{D}$ by $\iota : \partial\mathbb{D} \to \mathbb{D}$, we obtain the diagram in the middle. Passing through homology, we see that $H_1(\partial\mathbb{D})$ is isomorphic to $\mathbb{F}_2$, i.e., it has rank 1, while $H_1(\mathbb{D}) = 0$. But, as shown to the right, identity on the homology of $\partial\mathbb{D}$ maps each element to itself, while the second map on the bottom is injective, mapping 0 to exactly one element. Hence, the diagram to the right does not commute, i.e., $H_1(r) \circ H_1(\iota)(1) \neq \mathrm{Id}$, and we obtain a contradiction.

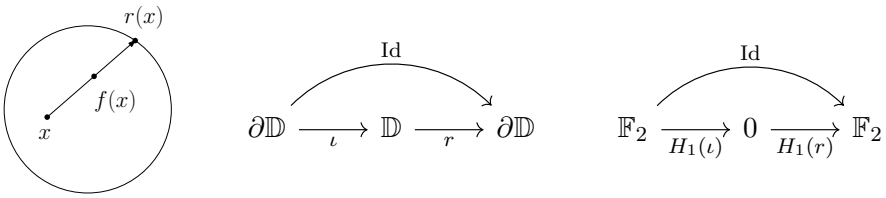

Fig. 13: Self-maps on the disk $\mathbb{D}$ with no fixed points, and a contradiction through functoriality.

The proof above generalizes to higher dimensions; for $\mathbb{D}^n$ we use H_{n-1}. This theorem is closely related to the *hairy ball theorem* establishing the impossibility of continuous and everywhere non-vanishing tangent vector fields on an even-dimensional sphere: *you can't comb the hair on a coconut!*

Beyond the surfaces we have been using in our elementary introduction, data analysis applications frequently deal with *sample points* assumed to be drawn from an *unknown* underlying manifold embedded in high dimensional space $\mathbb{R}^d$. We conclude with a brief discussion of how the techniques from above can be applied in this context, as has recently been in rapid development in the computational topology and topological data analysis research communities.

A major thrust in the development of topological approaches to data analysis is to achieve robustness against errors and imprecision in data measurements, collectively referred to as *noise*. As we have seen, topological properties are less sensitive to exact distances, which can be useful in the derivation of robust qualitative descriptors.

Homotopy Equivalence. An intuitive way to *hallucinate* the whole of a shape from a collection of sample points is to *grow* a ball around each sample and take the union of those balls. While this seems to work visually, there is a technical complication we need to consider. For example, if we take a dense sample on a 1-dimensional curve, grow a ball at each sample and take the union, we obtain a *thick* version of the curve; a tube of sorts. While the tube can be deformed continuously into the original curve, it would not be possible to define a continuous inverse, since many points on the tube will have to be mapped to the same point on the curve. Still, we would expect the union of balls to capture the topology of the original shape. This generalized notion of topological equivalence is called *homotopy equivalence*; while it is weaker form of equivalence compared to homeomorphism, it can be much more convenient.

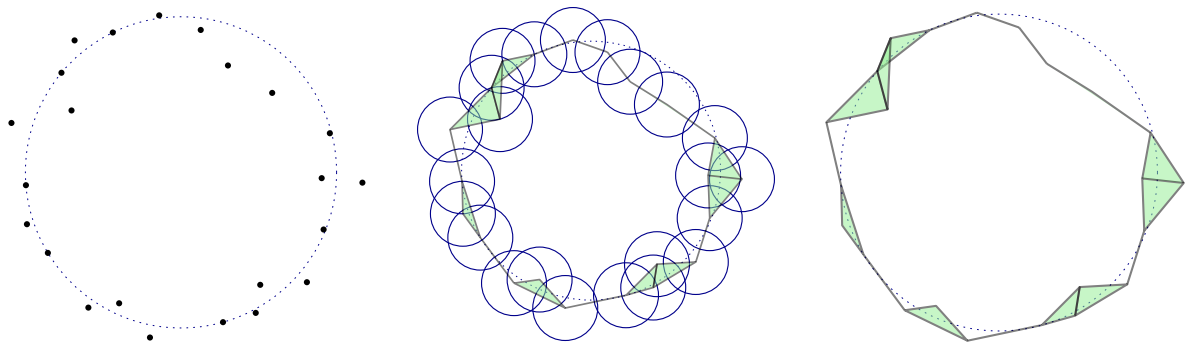

Fig. 14: Noisy samples from a circle, the union of balls and its nerve, and the Cêch complex.

Applying the idea outlined above, we work with the union of balls of a suitable radius. Unsurprisingly, we replace the geometric object represented by the union of balls by an algebraic object amenable to processing, i.e., a (abstract) simplicial complex.

Nerves. Taking the collection of balls centered at each sample point, we associate a vertex with each ball and a p-simplex with each subset of $(p+1)$ balls with a non-empty intersection. This type of complex is known as the *nerve* of the collection of objects; the balls in this case as shown in Figure 14. The homotopy-equivalence of this Cêch complex and the union of balls follows from the *nerve lemma*, which requires that the intersections of any set of objects is *contractible*, i.e., homotopy-equivalent to a point. This turns out to be the case for any collection of closed convex objects, not only balls, which can be related to *Helly's theorem*.

There remains the issue of choosing a suitable radius. In addition, the choice of radius is not completely separate from the density of the sample and the shape of the manifold. As the choice of radius impacts the topology type observed through the union of balls, how do we identify the most likely topology? This type of question motivated the recent development of a rich and exciting theory that came to be known as *persistent homology*.

To appreciate the issue of scale, we consider different choices of radii for the example in Figure 14.

Filtrations. As seen in Figure 15 below, a very small radius results in a disconnected union of balls, while an overly large radius yields a single blob with the hole *filled in*. Now, imagine a *continuous process* of growing the radii from $r = 0$ to $r = \infty$, where we think of r as a function of time t. As this process results in a sequence of nested shapes, it is called a *filtration*, with t being the *filtration parameter*. At some point, say $r(t_0) = a$, we recover the topology of the circle for the first time. Then, at a later point $t_1 > t_0$, with $r(t_1) = b > a$, the hole is filled in. Along the way, the number of connected components decreases as r goes from 0 to a.

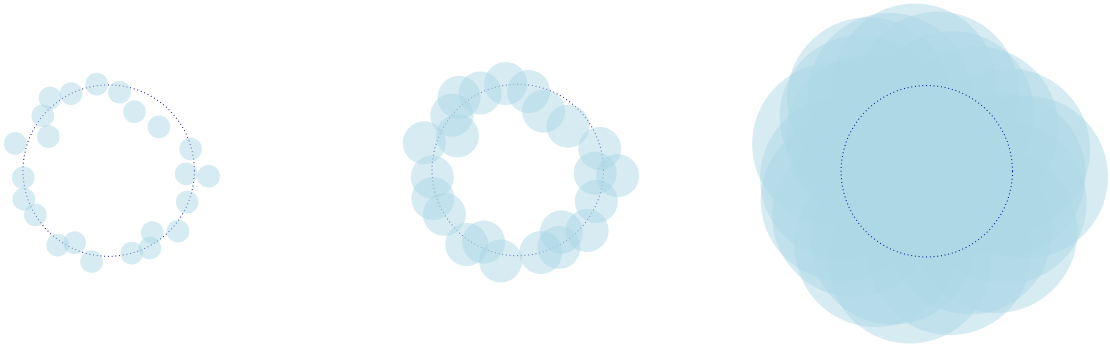

Fig. 15: Three different scales to estimate the topology from a noisy samples.

While filtrations provide a dynamical model of the evolution of topological features, we still need a way to extract the salient topological features as they appear and ultimately disappear. In addition, we would like to discard extraneous features arising due to the sampling and noise.

Persistence. We define the *birth* and *death* of a topological feature as the values of the filtration parameter when it first appears and when it gets filled in, respectively. Then, the *persistence* of the feature is the difference between the two. In the example above, the persistence of the 1-cycle is $t_1 - t_0$. Under reasonable conditions on the sampling, features with larger persistence are more likely to capture salient aspects of the underlying *shape of the data*, while features with small persistence can be disregarded, e.g., the many connected components in Figure 15.

Outlook. For this brief introduction, we did not cover the algorithmic aspects of computational topology. The matrix reduction algorithm was simply presented as a variant of Gaussian elimination, and we did not discuss the extensions needed to compute persistent homology. Other important considerations involve more compact complexes than the Cêch complex, e.g., the Vietoris-Rips complex, or the simplification of simplicial complexes to reduce their sizes without changing their homotopy type, as would be beneficial for efficient computation. Finally, the extracted persistent homology features can be summarized into convenient topological signatures, known as *persistence diagrams* and *barcodes*, with an associated metric structure such that it can be used to efficiently compare two data sets using their salient topological properties. We hope the reader will be excited to further explore these topics, while catching up on all the technical details that could not be presented here in more depth.

Example. Consider the diamond-shaped complex in Figure 16 below. We will use this complex to derive the boundary matrices and compute the Euler characteristic per Equation 6.

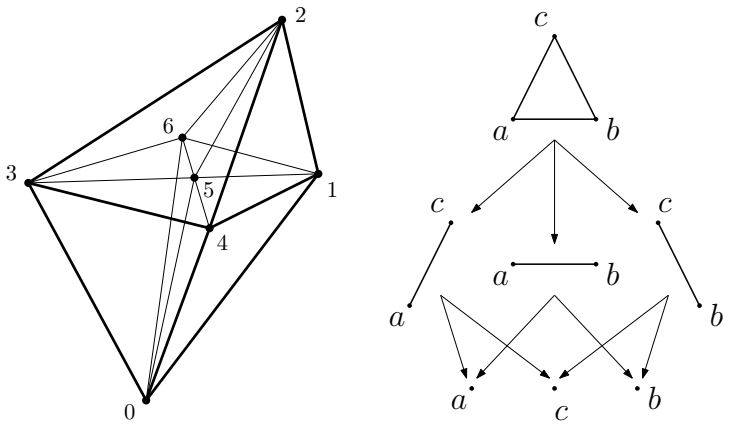

Fig. 16: A triangulation K of a diamond shape into eight tetrahedra, and a simple Hasse diagram.

To start, recall that the boundary map for vertices is simply the constant map to 0. We may express that in matrix form as:

$$\partial_0 = \begin{array}{c} \begin{matrix} 0 & 1 & 2 & 3 & 4 & 5 & 6 \end{matrix} \\ \begin{bmatrix} 0 & 0 & 0 & 0 & 0 & 0 & 0 \end{bmatrix} \end{array}$$

The first non-trivial boundary map is ∂_1 from edges to vertices. This boundary map is essentialy the *adjacency matrix* of the graph with the 0-simplices as its vertices and the 1-simplices as its edges. By examining the shape, the boundary matrix ∂_1 is readily produced. One can verify that the number of 1's in each column is exactly 2, while the number of 1's in each row is the degree of the node corresponding to that row.

$$\partial_1 = \begin{array}{c} \\ 0 \\ 1 \\ 2 \\ 3 \\ 4 \\ 5 \\ 6 \end{array} \begin{array}{c} \begin{matrix} \overline{01} & \overline{03} & \overline{04} & \overline{05} & \overline{06} & \overline{12} & \overline{14} & \overline{15} & \overline{16} & \overline{23} & \overline{24} & \overline{25} & \overline{26} & \overline{34} & \overline{35} & \overline{36} & \overline{45} & \overline{56} \end{matrix} \\ \begin{bmatrix} 1 & 1 & 1 & 1 & 1 & 0 & 0 & 0 & 0 & 0 & 0 & 0 & 0 & 0 & 0 & 0 & 0 & 0 \\ 1 & 0 & 0 & 0 & 0 & 1 & 1 & 1 & 1 & 0 & 0 & 0 & 0 & 0 & 0 & 0 & 0 & 0 \\ 0 & 0 & 0 & 0 & 0 & 1 & 0 & 0 & 0 & 1 & 1 & 1 & 1 & 0 & 0 & 0 & 0 & 0 \\ 0 & 1 & 0 & 0 & 0 & 0 & 0 & 0 & 0 & 1 & 0 & 0 & 0 & 1 & 1 & 1 & 0 & 0 \\ 0 & 0 & 1 & 0 & 0 & 0 & 1 & 0 & 0 & 0 & 1 & 0 & 0 & 1 & 0 & 0 & 1 & 0 \\ 0 & 0 & 0 & 1 & 0 & 0 & 0 & 1 & 0 & 0 & 0 & 1 & 0 & 0 & 1 & 0 & 1 & 1 \\ 0 & 0 & 0 & 0 & 1 & 0 & 0 & 0 & 1 & 0 & 0 & 0 & 1 & 0 & 0 & 1 & 0 & 1 \end{bmatrix} \end{array}$$

The remaining boundary maps ∂_2 and ∂_3 would take a bit more work, as shown in the next page. Instead of the graph analogy we used in deriving ∂_1, the simplicial structure of the complex as a whole can be represented in a *Hasse diagram*; see Figure 16 for an example. As a compact representation of the relationship between faces of all dimensions, Hasse diagrams can be processed to simplify a complex in order to reduce its size.

$$\partial_2 = \begin{array}{c|cccccccccccccccccccc} & \triangle 014 & \triangle 015 & \triangle 016 & \triangle 034 & \triangle 035 & \triangle 036 & \triangle 045 & \triangle 056 & \triangle 124 & \triangle 125 & \triangle 126 & \triangle 145 & \triangle 156 & \triangle 234 & \triangle 235 & \triangle 236 & \triangle 245 & \triangle 256 & \triangle 345 & \triangle 356 \\ \hline \overline{01} & 1 & 1 & 1 & & & & & & & & & & & & & & & & & \\ \overline{03} & & & & 1 & 1 & 1 & & & & & & & & & & & & & & \\ \overline{04} & 1 & & & 1 & & & 1 & & & & & & & & & & & & & \\ \overline{05} & & 1 & & & 1 & & 1 & 1 & & & & & & & & & & & & \\ \overline{06} & & & 1 & & & 1 & & 1 & & & & & & & & & & & & \\ \overline{12} & & & & & & & & & 1 & 1 & 1 & & & & & & & & & \\ \overline{14} & 1 & & & & & & & & 1 & & & 1 & & & & & & & & \\ \overline{15} & & 1 & & & & & & & & 1 & & 1 & 1 & & & & & & & \\ \overline{16} & & & 1 & & & & & & & & 1 & & 1 & & & & & & & \\ \overline{23} & & & & & & & & & & & & & & 1 & 1 & 1 & & & & \\ \overline{24} & & & & & & & & & 1 & & & & & 1 & & & 1 & & & \\ \overline{25} & & & & & & & & & & 1 & & & & & 1 & & 1 & 1 & & \\ \overline{26} & & & & & & & & & & & 1 & & & & & 1 & & 1 & & \\ \overline{34} & & & & 1 & & & & & & & & & & 1 & & & & & 1 & \\ \overline{35} & & & & & 1 & & & & & & & & & & 1 & & & & 1 & 1 \\ \overline{36} & & & & & & 1 & & & & & & & & & & 1 & & & & 1 \\ \overline{45} & & & & & & & 1 & & & & & 1 & & & & & 1 & & 1 & \\ \overline{56} & & & & & & & & 1 & & & & & 1 & & & & & 1 & & 1 \end{array}$$

$$\partial_3 = \begin{array}{c|cccccccc} & \triangle 0145 & \triangle 0156 & \triangle 0345 & \triangle 0356 & \triangle 1245 & \triangle 1256 & \triangle 2345 & \triangle 2356 \\ \hline \triangle 014 & 1 & & & & & & & \\ \triangle 015 & 1 & & 1 & & & & & \\ \triangle 016 & & 1 & & & & & & \\ \triangle 034 & & & 1 & & & & & \\ \triangle 035 & & & 1 & 1 & & & & \\ \triangle 036 & & & & 1 & & & & \\ \triangle 045 & 1 & & 1 & & & & & \\ \triangle 056 & & 1 & & 1 & & & & \\ \triangle 124 & & & & & 1 & & & \\ \triangle 125 & & & & & 1 & 1 & & \\ \triangle 126 & & & & & & 1 & & \\ \triangle 145 & 1 & & & & 1 & & & \\ \triangle 156 & & 1 & & & & 1 & & \\ \triangle 234 & & & & & & & 1 & \\ \triangle 235 & & & & & & & 1 & 1 \\ \triangle 236 & & & & & & & & 1 \\ \triangle 245 & & & & & 1 & & 1 & \\ \triangle 256 & & & & & & 1 & & 1 \\ \triangle 345 & & & 1 & & & & 1 & \\ \triangle 356 & & & & 1 & & & & 1 \end{array}$$

Using the matrix reduction algorithm, we can reduce the matrices as shown below.

$$\text{Reduce}(\partial_0) = \begin{bmatrix} 0 & 0 & 0 & 0 & 0 & 0 & 0 \end{bmatrix},$$

$$\text{Reduce}(\partial_1) = \begin{bmatrix}
1 & 0 & 0 & 0 & 0 & 0 & 0 & 0 & 0 & 0 & 0 & 0 & 0 & 0 & 0 & 0 & 0 & 0 \\
0 & 1 & 0 & 0 & 0 & 0 & 0 & 0 & 0 & 0 & 0 & 0 & 0 & 0 & 0 & 0 & 0 & 0 \\
0 & 0 & 1 & 0 & 0 & 0 & 0 & 0 & 0 & 0 & 0 & 0 & 0 & 0 & 0 & 0 & 0 & 0 \\
0 & 0 & 0 & 1 & 0 & 0 & 0 & 0 & 0 & 0 & 0 & 0 & 0 & 0 & 0 & 0 & 0 & 0 \\
0 & 0 & 0 & 0 & 1 & 0 & 0 & 0 & 0 & 0 & 0 & 0 & 0 & 0 & 0 & 0 & 0 & 0 \\
0 & 0 & 0 & 0 & 0 & 1 & 0 & 0 & 0 & 0 & 0 & 0 & 0 & 0 & 0 & 0 & 0 & 0 \\
0 & 0 & 0 & 0 & 0 & 0 & 0 & 0 & 0 & 0 & 0 & 0 & 0 & 0 & 0 & 0 & 0 & 0
\end{bmatrix},$$

$$\text{Reduce}(\partial_2) = \begin{bmatrix}
1 & 0 & 0 & 0 & 0 & 0 & 0 & 0 & 0 & 0 & 0 & 0 & 0 & 0 & 0 & 0 & 0 & 0 & 0 & 0 \\
0 & 1 & 0 & 0 & 0 & 0 & 0 & 0 & 0 & 0 & 0 & 0 & 0 & 0 & 0 & 0 & 0 & 0 & 0 & 0 \\
0 & 0 & 1 & 0 & 0 & 0 & 0 & 0 & 0 & 0 & 0 & 0 & 0 & 0 & 0 & 0 & 0 & 0 & 0 & 0 \\
0 & 0 & 0 & 1 & 0 & 0 & 0 & 0 & 0 & 0 & 0 & 0 & 0 & 0 & 0 & 0 & 0 & 0 & 0 & 0 \\
0 & 0 & 0 & 0 & 1 & 0 & 0 & 0 & 0 & 0 & 0 & 0 & 0 & 0 & 0 & 0 & 0 & 0 & 0 & 0 \\
0 & 0 & 0 & 0 & 0 & 1 & 0 & 0 & 0 & 0 & 0 & 0 & 0 & 0 & 0 & 0 & 0 & 0 & 0 & 0 \\
0 & 0 & 0 & 0 & 0 & 0 & 1 & 0 & 0 & 0 & 0 & 0 & 0 & 0 & 0 & 0 & 0 & 0 & 0 & 0 \\
0 & 0 & 0 & 0 & 0 & 0 & 0 & 1 & 0 & 0 & 0 & 0 & 0 & 0 & 0 & 0 & 0 & 0 & 0 & 0 \\
0 & 0 & 0 & 0 & 0 & 0 & 0 & 0 & 1 & 0 & 0 & 0 & 0 & 0 & 0 & 0 & 0 & 0 & 0 & 0 \\
0 & 0 & 0 & 0 & 0 & 0 & 0 & 0 & 0 & 1 & 0 & 0 & 0 & 0 & 0 & 0 & 0 & 0 & 0 & 0 \\
0 & 0 & 0 & 0 & 0 & 0 & 0 & 0 & 0 & 0 & 1 & 0 & 0 & 0 & 0 & 0 & 0 & 0 & 0 & 0 \\
0 & 0 & 0 & 0 & 0 & 0 & 0 & 0 & 0 & 0 & 0 & 1 & 0 & 0 & 0 & 0 & 0 & 0 & 0 & 0 \\
0 & 0 & 0 & 0 & 0 & 0 & 0 & 0 & 0 & 0 & 0 & 0 & 0 & 0 & 0 & 0 & 0 & 0 & 0 & 0 \\
0 & 0 & 0 & 0 & 0 & 0 & 0 & 0 & 0 & 0 & 0 & 0 & 0 & 0 & 0 & 0 & 0 & 0 & 0 & 0 \\
0 & 0 & 0 & 0 & 0 & 0 & 0 & 0 & 0 & 0 & 0 & 0 & 0 & 0 & 0 & 0 & 0 & 0 & 0 & 0 \\
0 & 0 & 0 & 0 & 0 & 0 & 0 & 0 & 0 & 0 & 0 & 0 & 0 & 0 & 0 & 0 & 0 & 0 & 0 & 0 \\
0 & 0 & 0 & 0 & 0 & 0 & 0 & 0 & 0 & 0 & 0 & 0 & 0 & 0 & 0 & 0 & 0 & 0 & 0 & 0 \\
0 & 0 & 0 & 0 & 0 & 0 & 0 & 0 & 0 & 0 & 0 & 0 & 0 & 0 & 0 & 0 & 0 & 0 & 0 & 0
\end{bmatrix},$$

$$\text{Reduce}(\partial_3) = \begin{bmatrix}
1 & 0 & 0 & 0 & 0 & 0 & 0 & 0 \\
0 & 1 & 0 & 0 & 0 & 0 & 0 & 0 \\
0 & 0 & 1 & 0 & 0 & 0 & 0 & 0 \\
0 & 0 & 0 & 1 & 0 & 0 & 0 & 0 \\
0 & 0 & 0 & 0 & 1 & 0 & 0 & 0 \\
0 & 0 & 0 & 0 & 0 & 1 & 0 & 0 \\
0 & 0 & 0 & 0 & 0 & 0 & 1 & 0 \\
0 & 0 & 0 & 0 & 0 & 0 & 0 & 1 \\
0 & 0 & 0 & 0 & 0 & 0 & 0 & 0 \\
\vdots & \vdots & \vdots & \vdots & \vdots & \vdots & \vdots & \vdots \\
0 & 0 & 0 & 0 & 0 & 0 & 0 & 0
\end{bmatrix}.$$

From the reduced matrices, we extract the ranks of the boundary and cycle groups:

p	rank Z_p	rank B_p
0	7	6
1	12	8
2	12	0
3	8	0

Using the ranks, we can now compute the Euler characteristic by substituting into Equation 6

$$\begin{aligned}\chi &= \sum_{p\geq 0}(-1)^p\beta_i \\ &= \sum_{p\geq 0}(-1)^p(\text{rank } Z_p - \text{rank } B_p) \\ &= (7-6)-(12-8)+(12-0)-(8-0) \\ &= 1.\end{aligned}$$

The following exercise demonstrates the invariance of the Euler characteristic if we use a different triangulation of the diamond shape. In addition, to better distinguish the Euler characteristic of the sphere from that of the ball, we also consider a triangulation of only the boundary of the diamond shape.

Exercise. Referring to Figure 17 below, verify that $\chi(K_2) = 1$ and $\chi(K') = 2$.

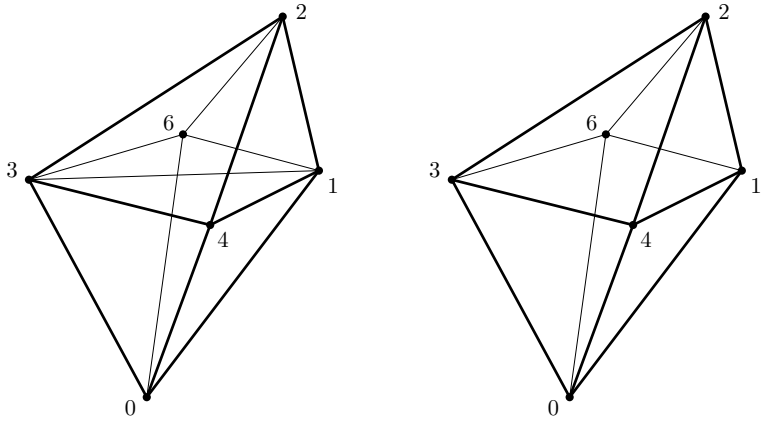

(a) K_2. (b) K'.

Fig. 17: Two different triangulations related to the example in Figure 16.